Supporting Information

MoS_2-based dual-responsive flexible anisotropic actuators

Zhouyue Lei,[a] *Wencheng Zhu,*[b] *Shengtong Sun*[*c] *and Peiyi Wu*[*a]

a. State Key Laboratory of Molecular Engineering of Polymers, Collaborative Innovation Center of Polymers and Polymer Composite Materials, Department of Macromolecular Science and Laboratory for Advanced Materials, Fudan University, Shanghai 200433, China. Email: peiyiwu@fudan.edu.cn

b. Institute of Biochemistry and Cell Biology, Shanghai Institutes for Biological Sciences, Chinese Academy of Sciences, Shanghai 200031, China.、

c. School of Chemical Engineering, State Key Laboratory of Chemical Engineering, Shanghai Key Laboratory of Multiphase Materials Chemical Engineering, East China University of Science and Technology, 130 Meilong Road, Shanghai 200237, China
Email: shengtongsun@ecust.edu.cn

Calculation of the photothermal conversion efficiency

Photothermal conversion efficiency of the chitosan-coated MoS_2 nanosheets was calculated based on the dispersion with the concentration of 320 μg mL^{-1} upon NIR irradition (808 nm, 2.5 W cm^{-2}).

According to previous reports,[1, 2] the photothermal conversion efficiency (η) of chitosan-functionalized MoS_2 nanosheets can be calculated based on following Equation 1,

$$\eta = \frac{hS\,(T_{max} - T_{surr}) - Q_{Dis}}{I\,(1 - 10^{-A808})} \quad (1)$$

in which h (mW m^{-2} $^{o}C^{-1}$) is heat transfer coefficient, S (m^2) the surface area of the quartz cuvette container, T_{max} the maximum equilibrium temperature, T_{Surr} ambient temperature of the surroundings, Q_{Dis} the heat dissipated from light absorbed by the quartz sample cell itself, I (1 W) the laser power and A_{808} the absorbance of the nanosheets at the wavelength of 808 nm.

In order to get the hS, a sample system time constant τ_s and a dimensionless driving force temperature θ are introduced,

$$\tau_s = \frac{\sum_i m_i C_{p,i}}{hS} \quad (2)$$

$$\theta = \frac{T - T_{surr}}{T_{max} - T_{surr}} \quad (3)$$

where m_i and $C_{p,i}$ correspond the mass and heat capacity, respectively.

Based on total energy balance of the system, Equation 3 can be rearranged as

$$\frac{d\theta}{dt} = \frac{1}{\tau_s}\left[\frac{Q_{laser}}{hS\,(T_{max} - T_{surr})} - \theta\right] \quad (4)$$

when the light source is shut off, the Q_{laser} is 0 at the cooling stage of the aqueous dispersion, therefore, the Equation (4) can be expressed as

$$dt = -\tau_s \frac{d\theta}{\theta} \quad (5)$$

after integrating, it gives the expression of Equation (6),

$t = -\tau_s ln\theta$ (6)

According to the linear time data derived from the cooling period time, the heat transfer of the system is determined to be τ_s = 392.21 s. Therefore, by substituting the m_s (0.991 g), m_c (4.838 g), $C_{p,c}$ (0.839 J $g^{-1}K^{-1}$) and the $C_{p,s}$ (4.187 J $g^{-1}K^{-1}$) in Equation 2, hS is deduced to be 20.93 mW K^{-1}. Finally, the photothermal conversion efficiency (η) was calculated to be 47%.

Curvature change of hydrogel actuators

Curvature of hydrogel actuators was calculated through Equation (7):

$$\frac{1}{r} = \frac{2\pi\theta}{360L} \quad (7)$$

in which $\frac{1}{r}$ corresponds to the curvature, r the radius, θ central angle, L the length of the hydrogel actuator arm (14 mm). The curvature change is the difference of curvatures at different stages.

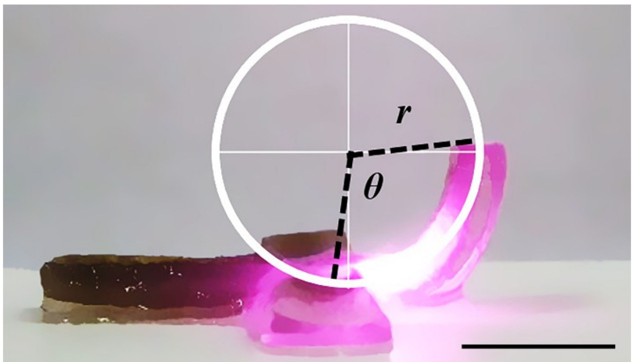

Fig. S1 Measuring the central angle (θ, degree) of the hydrogel actuator (scale bar: 1 cm).

Evaluation of the shape fixity ratio and the shape recovery ratio

The deformation of the hydrogel actuators were recorded with a digital camera. The shape fixity ratio is calculated according to Equation (8)[3]:

$$F(t) = \frac{C(t) - C_0}{C_b - C_0} \times 100\% \quad (8)$$

in which C_0 is the original curvature, C_b the bending curvature, and $C(t)$ the time-dependent curvature of the hydrogel after switching the laser off.

The shape recovery ratio was calculated according to Equation (9)[3]:

$$R = \frac{C_b - C_r}{C_b - C_0} \times 100\% \qquad (9)$$

where C_r is the curvature of hydrogel actuator after recovery.

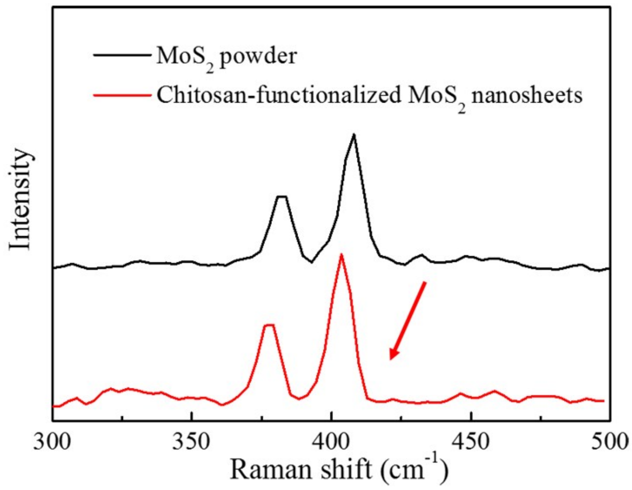

Fig. S2 Raman spectra of the bulk MoS_2 powder and chitosan-functionalized MoS_2 nanosheets.

Fig. S3 A typical photograph of the as-prepared chitosan-functionalized MoS_2 nanosheet dispersion after storage for six months.

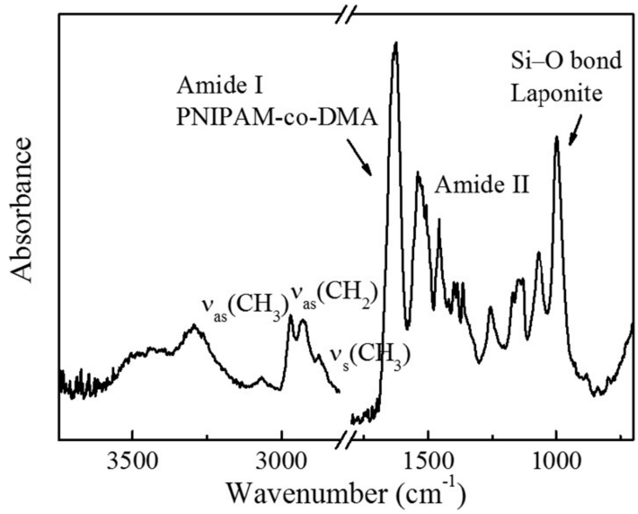

Fig. S4 FTIR spectrum of the MoS_2/PNIPAM-co-DMA composite hydrogel (the molar ratio of NIPAM and DMA is 3:1).

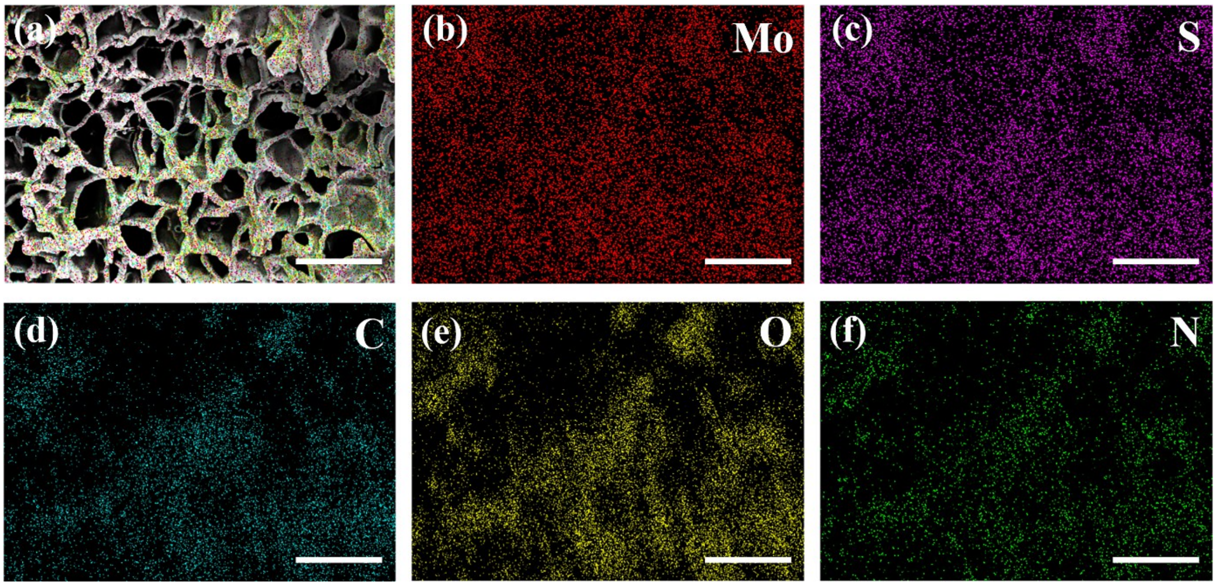

Fig. S5 (a) FESEM image and (b-f) corresponding element mapping images of the freeze-dried MoS_2/PNIPAM-co-DMA hydrogel (scale bar: 2.5 μm).

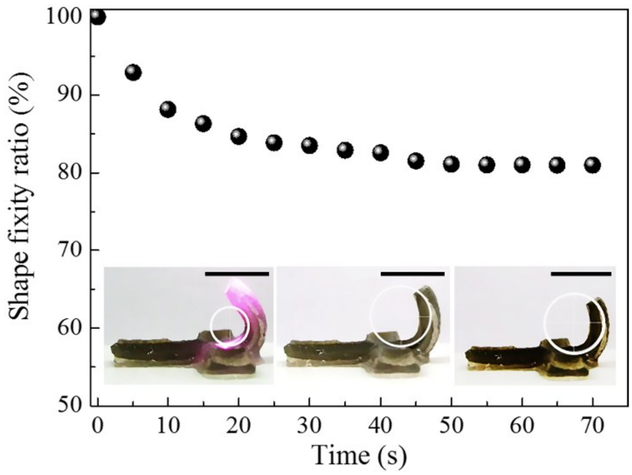

Fig. S6 Time-dependent shape fixity ratio of the anisotropic hydrogel actuator after switching off the laser and typical photographs recorded after 0, 35 and 70 s (scale bar: 1 cm).

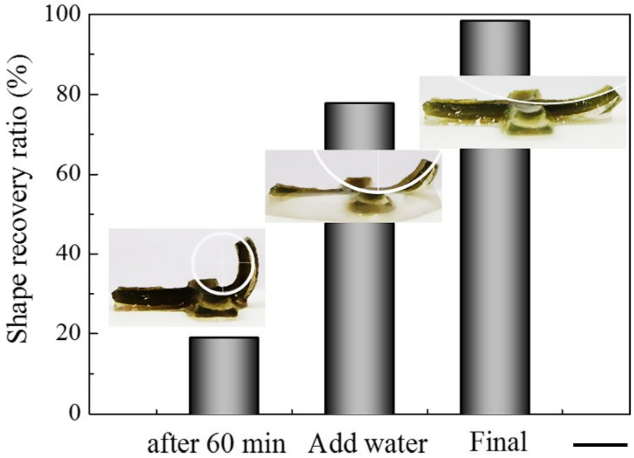

Fig. S7 Shape recovery ratio of the anisotropic hydrogel actuator and typical photographs recorded after switching off the laser for 60 min and adding a little water on the curved arm (scale bar: 1 cm).

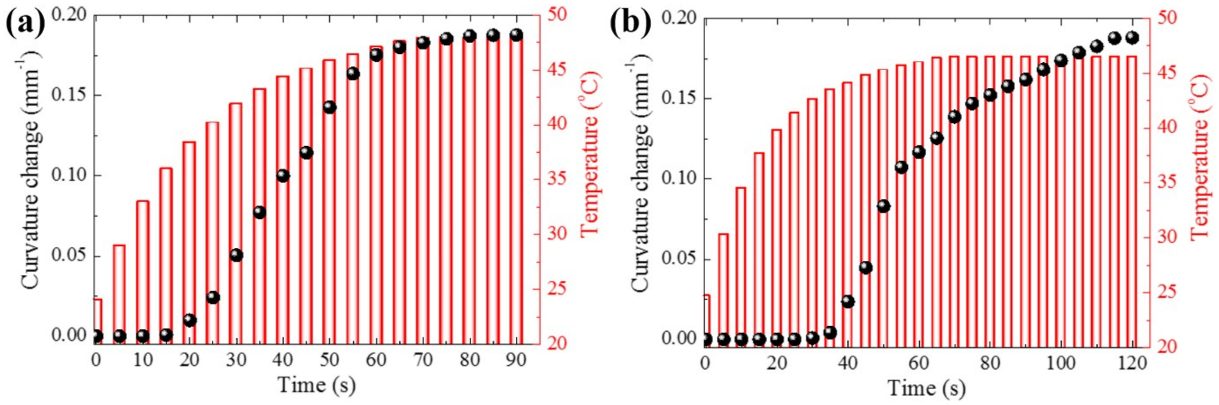

Fig. S8 Plots of curvature change (mm^{-1}) and temperature of the hydrogel actuator upon NIR irradiation with a power density of (a) 3.75 and (b) 2.5 Wcm^{-2}.

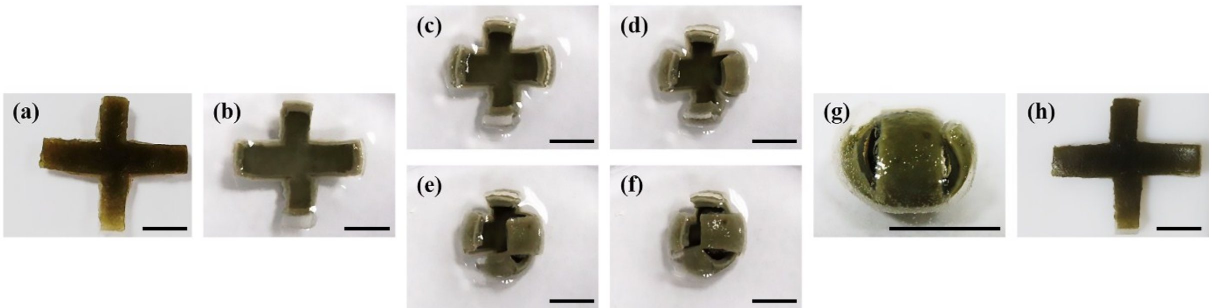

Fig. S9 Typical photographs of the anisotropic hydrogel actuator recorded (a) at room temperature and in hot water (70 °C) after (b) 1 s and (c-f) every 10 s. (g) is the final folded state in hot water and (h) is the recovered state at room temperature (scale bar: 1 cm).

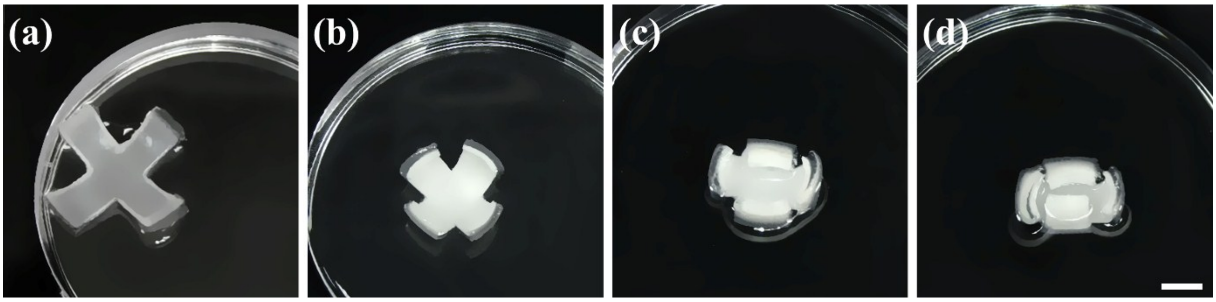

Fig. S10 Photographs of an anisotropic hydrogel (without MoS_2 nanosheets) in hot water (70 °C) after (a) 1, (b) 10, (c) 20 and (d) 30 s (scale bar: 1 cm).

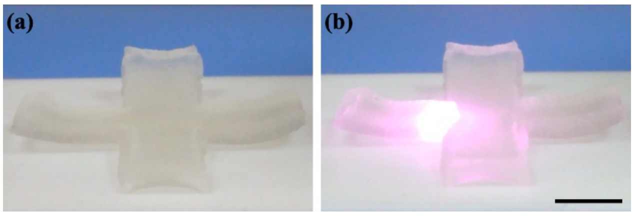

Fig. S11 Photographs of an anisotropic hydrogel (without MoS_2 nanosheets) at room temperature upon NIR irradiation (808 nm, 5 Wcm^{-2}) after (a) 0 and (b) 20 min (scale bar: 1 cm).

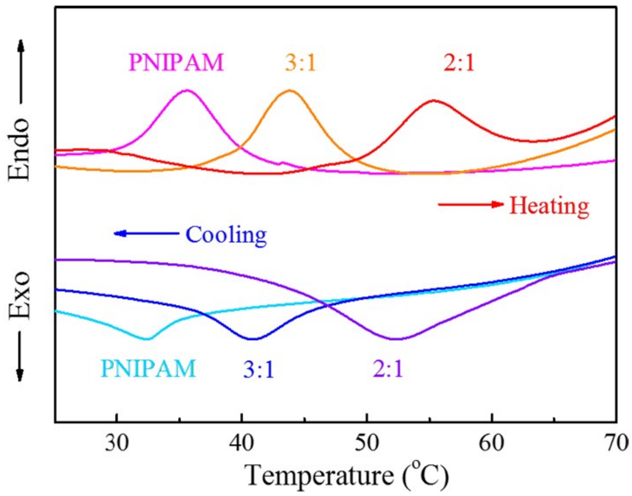

Fig. S12 DSC heating and cooling curves of the anisotropic hydrogel with different molar ratios of NIPAM and DMA in its first layer.

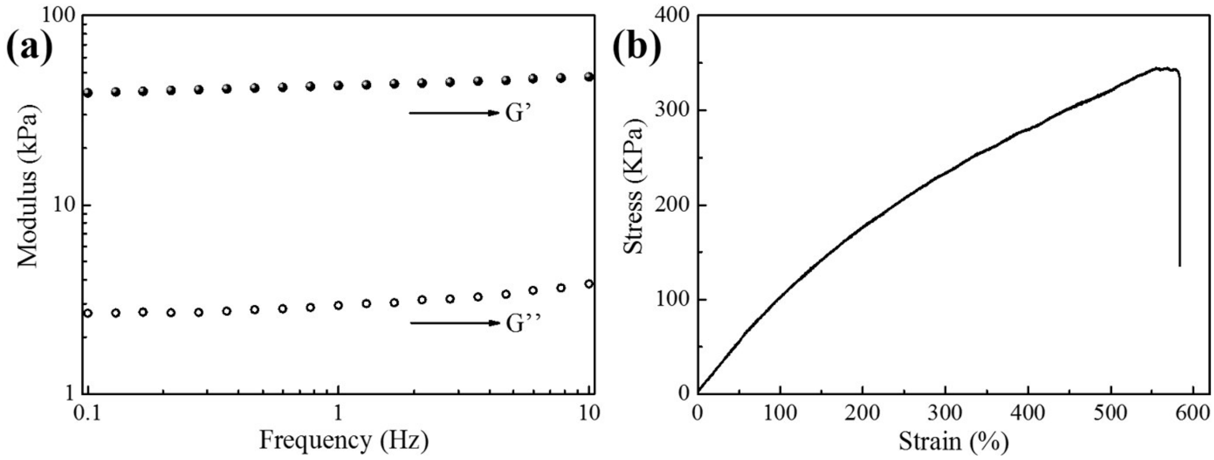

Fig. S13 (a) Frequency sweeps (dynamic mechanical measurement) of the anisotropic hydrogel, in which solid spheres represent storage modulus (G') and hollow spheres represent loss modulus (G''). (b) Tensile stress–strain curve of the anisotropic hydrogel.

References

1. D. K. Roper, W. Ahn and M. Hoepfner, *J. Phys. Chem. C*, 2007, **111**, 3636-3641.
2. H. Chen, L. Shao, T. Ming, Z. Sun, C. Zhao, B. Yang and J. Wang, *Small*, 2010, **6**, 2272-2280.
3. J. Hao and R. A. Weiss, *ACS Macro Lett.*, 2013, **2**, 86-89.